

Generation of frequency-correlated narrowband biphotons from four-wave mixing in cold atomsSujun Yun,¹ Jianming Wen,^{1,2,*} P. Xu,^{1,†} Min Xiao,^{1,2} and S.-N. Zhu¹¹*Department of Physics, National Laboratory of Solid State Microstructures, Nanjing University, Nanjing 210093, China*²*Department of Physics, University of Arkansas, Fayetteville, Arkansas 72701, USA*

(Received 24 September 2010; published 27 December 2010)

Generation of frequency-correlated narrowband biphotons from the four-wave mixing process is theoretically analyzed through manipulating optical properties of light propagation inside a cold atomic ensemble. In contrast with the spontaneous parametric down-conversion case, we find a much looser condition, which allows producing such frequency-correlated paired photons. We propose a two-photon temporal conditional correlation measurement to detect these photons. In addition, our results provide other evidence for observing backward pulse propagation from the viewpoint of two-photon correlation measurement.

DOI: [10.1103/PhysRevA.82.063830](https://doi.org/10.1103/PhysRevA.82.063830)

PACS number(s): 42.65.Lm, 42.50.Dv, 42.50.Gy, 42.25.Bs

I. INTRODUCTION

The field of quantum optics has witnessed significant developments in recent years, from the laboratory realization of counterintuitive concepts, such as quantum entanglement and Schrödinger cat states, to the investigation of novel technologies, such as quantum-information processing, quantum communication, quantum cryptography, and quantum imaging. To advance the progress in these fields, it is a primary task to have a good light source, which can emit entangled photons with some desirable joint wave forms. Conventionally, entangled photon pairs are produced from the process of spontaneous parametric down-conversion (SPDC) [1] in a nonlinear crystal in which an input pump photon is annihilated while two daughter photons are simultaneously created. Because of the energy conservation, these SPDC photons are usually frequency anticorrelated by assuming the input pump beam is a plane wave. For example, in the degenerate case, if the central frequency of one down-converted SPDC photon is tuned to a higher frequency, the central frequency of its twin photon must be shifted to a lower frequency. Because of their short coherence time, shaping the joint spectrum is implemented through spatial modulation of the nonlinear interaction [2–4], employing a pulsed pump laser [5], or modifying the phase-matching conditions [6]. With the extended-phase-matching conditions, the frequency-correlated entangled photons, especially the coincident-frequency photons [7], have been put forward. In contrast with frequency-anticorrelated paired photons, detecting one of these frequency-correlated photons with blue detuning from the central frequency implies that its twin is also blue detuned from the central frequency. Generating frequency-correlated biphotons with a few femtoseconds of correlation time is particularly useful for quantum metrology and timing and positioning measurements [8].

Recent demonstrations for generating entangled photon pairs from four-wave mixing (FWM) in cold atoms [9–13] exhibit a number of interesting properties, such as long coher-

ence time, long coherence length, high conversion efficiency, and high spectral brightness. More importantly, these photons are more suitable for long-distance quantum communication and quantum-information processing based on the interface of coherent interaction between atoms and photons than SPDC photons. Such a source also offers a flexible way to shape the two-photon wave form directly in the time domain. For instance, by encoding the information into the input beam profiles, it can be revealed in the two-photon coincidence measurements as theoretically proposed in Ref. [14] and experimentally demonstrated in Ref. [15]. Another example [16] is to engineer a biphoton spectrum through an electromagnetically induced grating [17], in which the directionality and spectral brightness of entangled paired photons can be enhanced further.

Despite this rapid progress, there is no report on generating frequency-correlated narrowband biphotons through FWM in a cold atomic system. We, therefore, wish to perform such a theoretical analysis here and show the feasibility of producing these photons in the current laboratory. We notice that frequency-correlated paired photons can, in principle, be created through FWM in a nonlinear optical fiber [18]. However, no experimental illustration has been reported to date, partly due to the difficulty of achieving the so-called extended-phase-matching conditions [7]. Frequency-correlated entangled photon pairs have been demonstrated with the use of a type-II periodically poled KTiOPO₄ [6], but the experiment severely depends on such a specially designed nonlinear crystal that its dispersive properties can satisfy the extended-phase matching. In contrast, biphoton generation from cold atoms via FWM offers much flexibility. That is, the dispersive properties of the system are tunable in a large range by manipulating experimental parameters. In our results, one noticeable difference from previous research [7] is that the extended-phase-matching condition is greatly loosened. This allows one to obtain frequency-correlated photons with less constraints. To detect these photons, we propose a two-photon temporal correlation measurement conditioned on the trigger of the input probe pulse. Moreover, our results also suggest other evidence for observing backward pulse propagation from the viewpoint of the two-photon correlation measurement.

We organize our paper as follows. To be specific, we take a four-level double- Λ cold atomic system to illustrate the

*jianming.wen@gmail.com

†pingxu520@nju.edu.cn

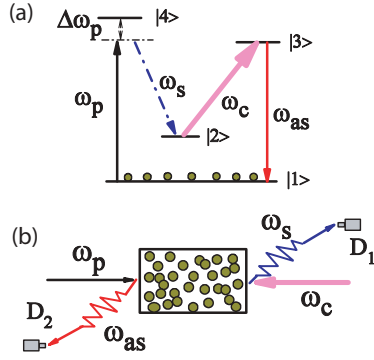


FIG. 1. (Color online) (a) Atomic level structure for generating frequency-correlated Stokes-anti-Stokes photons. (b) Simplified experimental setup. By applying the probe and control fields in the counterpropagation configuration, paired Stokes-anti-Stokes photons simultaneously are produced and detected by two single-photon detectors, D_1 and D_2 , in the backward geometry.

basic idea. In Sec. II, we look at the dispersive properties of the ensemble for the corresponding electromagnetic fields. In Sec. III, the two-photon state is calculated in first-order perturbation theory. We give a more general condition, which allows generating the frequency-correlated paired photons. In Sec. IV, we consider the two-photon temporal correlation in coincidence-counting measurements. Finally, we give our concluding remarks.

II. DISPERSIVE PROPERTIES OF THE ATOMIC SYSTEM

For simplicity, we consider a four-level double- Λ system, which consists of identical atoms with length L and the average atomic density N . Initially, all the population is distributed in their ground state $|1\rangle$, as shown in Fig. 1(a). Paired Stokes and anti-Stokes photons are generated backward as applying one weak probe and one strong control beam in the counterpropagation geometry, as depicted in Fig. 1(b). Here, the weak probe field is assumed to be a pulsed laser, which is off-resonant with atomic transition $|1\rangle \rightarrow |4\rangle$; while the strong control light is a cw laser, which is on-resonance with transition $|2\rangle \rightarrow |3\rangle$. We denote the angular frequency of each field as ω_j and the wave number as k_j ($j = s, as, p, c$). As shown in Fig. 1(b), paired Stokes and anti-Stokes photons are produced and are detected by two single-photon detectors, D_1 and D_2 , in the backward-propagation configuration. Since the atoms are laser cooled and trapped, the Doppler broadening is negligible and will not be taken into account.

To look at the generation of frequency-correlated paired photons, it is instructive to start with the optical response of the medium for the fields, which are involved in the interaction. Following the analysis presented in Ref. [19], the third-order nonlinear susceptibility for the generated anti-Stokes field takes the form

$$\chi_{as}^{(3)} = \frac{N\hbar d_{24}d_{13}d_{41}d_{32}}{\epsilon_0} \frac{1}{(\Gamma_{21}^* \Gamma_{as}^* - |\Omega_c|^2)\Gamma_p^*}, \quad (1)$$

and the linear susceptibilities for the pump, Stokes, and anti-Stokes fields are, respectively,

$$\begin{aligned} \chi_p &= \frac{N\hbar|d_{41}|^2}{\epsilon_0} \frac{1}{\Gamma_p}, \\ \chi_s &= \frac{N\hbar|d_{24}|^2}{\epsilon_0} \frac{|\Omega_p|^2\Gamma_{as}}{(\Gamma_{21}\Gamma_{as} - |\Omega_c|^2)\Gamma_s^*\Gamma_p^*}, \\ \chi_{as} &= \frac{N\hbar|d_{13}|^2}{\epsilon_0} \frac{\Gamma_{21}^*}{\Gamma_{21}^*\Gamma_{as}^* - |\Omega_c|^2}. \end{aligned} \quad (2)$$

Here, the complex detunings are defined as $\Gamma_p = \omega_{41} - \omega_p + i\gamma_{41}$, $\Gamma_s = \omega_{42} - \omega_s + i\gamma_{42}$, $\Gamma_{as} = \omega_{31} - \omega_{as} + i\gamma_{31}$, and $\Gamma_{21} = \omega_{21} - \omega_p + \omega_s + i\gamma_{21}$, where ω_{ij} ($i, j = 1, 2, 3, 4$) is the atomic transition frequency between levels $|i\rangle$ and $|j\rangle$, $d_{ij} = \frac{e\langle i|r|j\rangle}{\hbar}$ stands for the dipole matrix element divided by \hbar , and γ_{ij} represents the decay or dephasing rate. $\Omega_{p(c)}$ is the probe or control Rabi frequency. The physics behind $\chi_{as}^{(3)}$ has been addressed in Ref. [11], which will not be repeated here. In fact, for generating frequency-correlated paired photons, the linear optical responses described by Eq. (2) play an indispensable role in the process. Hence, in the following, we will focus on these linear susceptibilities.

It is well known that the real part of the linear susceptibility determines the dispersion of the material, while the imaginary part controls the transmission and absorption. From Eq. (2), it is not difficult to find the group velocities of the probe and anti-Stokes fields, respectively, within the ensemble,

$$u_p \approx -\frac{2\epsilon_0 c \gamma_{41}^2}{N\hbar|d_{41}|^2 \omega_{41}}, \quad (3)$$

$$u_{as} \approx \frac{2\epsilon_0 c |\Omega_c|^2}{N\hbar|d_{31}|^2 \omega_{31}}. \quad (4)$$

In contrast, the Stokes and control fields propagate inside the atoms at almost the speed of light in vacuum, c . It is clear from Eq. (3) that the probe field traverses the medium with a negative (or superluminal) group velocity because of a small amount of population inversion and reshaping of the profile [20]. We notice that such an exotic propagation effect, backward pulse propagation, has been previously observed in the experiment [21]. Our results obtained here, thus, provide other evidence for observing such an effect from the viewpoint of the two-photon correlation measurement. Instead, the anti-Stokes field passes through the system with a slow group velocity due to the slow-light effect of electromagnetically induced transparency [22]. To get a feeling of the magnitude of these quantities, let us take the ^{87}Rb D_2 line [23] as an example. If $N \sim 10^{12}$ atoms/cm³ and $\Omega_c \sim 2 \times 10^7$ Hz, one then has $u_p \sim -2000$ m/s and $u_{as} \sim 240$ m/s.

III. TWO-PHOTON STATE

To describe the state of paired Stokes-anti-Stokes photons, we work in the interaction picture. The effective Hamiltonian is given by

$$H_I = \epsilon_0 \int_{-L}^0 dz \chi_{as}^{(3)} \hat{E}_p^{(+)} \hat{E}_c^{(+)} \hat{E}_s^{(-)} \hat{E}_{as}^{(-)} + \text{H.c.}, \quad (5)$$

where H.c. means the Hermitian conjugate. As usual, the weak pulsed probe and strong cw control beams are taken as classical

electric fields, while the new fields, Stokes and anti-Stokes, are treated quantum mechanically. That is,

$$\begin{aligned}
 E_p &= \int dv_p \tilde{E}_p(v_p) e^{i(k_p z - v_p t)} e^{-i\varpi_p t}, \\
 E_c &= E_c e^{-i(k_c z + \omega_c t)}, \\
 \hat{E}_s^{(+)} &= \sum_{k_s} \varepsilon_s \hat{a}_s e^{i(k_s z - \omega_s t)}, \\
 \hat{E}_{as}^{(+)} &= \sum_{k_{as}} \varepsilon_{as} \hat{a}_{as} e^{-i(k_{as} z + \omega_{as} t)},
 \end{aligned} \quad (6)$$

where ϖ_p is the central frequency of the probe field, $\tilde{E}_p(v_p)$ is its spectral profile, and $\varepsilon_j = i\sqrt{\hbar\omega_j/2\epsilon_0 n_j^2 V_q}$ ($j = s, as$) with the refraction index n_j and quantization volume V_q .

With the use of Eqs. (5) and (6), the two-photon state can then be evaluated from first-order perturbation theory [24], which gives [11,19]

$$\begin{aligned}
 |\Psi\rangle &= A \int d\omega_s \int d\omega_{as} \int dv_p \tilde{E}(v_p) \chi_{as}^{(3)} \Phi(\Delta_k L) \\
 &\quad \times \delta(\varpi_p + v_p + \omega_c - \omega_s - \omega_{as}) \hat{a}^\dagger(\omega_s) \hat{a}^\dagger(\omega_{as}) |0\rangle,
 \end{aligned} \quad (7)$$

where all the slowly varying terms and constants are absorbed into A and the summations have been converted into the angular frequencies. In Eq. (7), $\Phi(x) = \text{sinc}(\frac{x}{2})e^{-i(x/2)}$ is the joint natural spectrum function of the photons, which carries the information of the phase mismatching Δ_k in the longitudinal direction over the whole interaction length. The Dirac δ function implies that the energy conservation is well satisfied in the FWM process. One may notice that, different from previous research [11,19], Eq. (7) involves one more integration over the spectrum of the probe field. Although the δ function allows the elimination of one integral, two integrals still survive in Eq. (7), which may result in the deduction of the degree of entanglement between two particles [5]. In fact, a maximally entangled state is still available if one forces the joint spectrum function Φ to approach a Dirac δ function, as first noted by Giovannetti and his co-workers [7]. This observation leads to the generation of frequency-correlated biphotons. Before proceeding with the discussion, we notice that, as previously addressed in Refs. [9,11–13], the efficiency of generating these photons can be made usually higher than that of SPDC [6]. Of course, here, the efficiency depends on the system parameters, such as the input beams power, the atomic density, and the detunings.

Following the treatment done in Ref. [7], we look at the joint natural spectrum function Φ first. In the counterpropagating geometry, the wave-number mismatch Δ_k in the first-order Taylor expansion with respect to their central frequencies ϖ_j can be recast into the following form:

$$\begin{aligned}
 \Delta_k &= \left(\frac{1}{u_p} + \frac{1}{u_{as}}\right)(\omega_{as} - \varpi_{as}) - \left(\frac{1}{c} - \frac{1}{u_p}\right)(\omega_s - \varpi_s) \\
 &= \left(\frac{1}{c} - \frac{1}{u_p}\right)[\beta(\omega_{as} - \varpi_{as}) - (\omega_s - \varpi_s)],
 \end{aligned} \quad (8)$$

where the group velocity of the Stokes field is simply taken as c . In Eq. (8), we have introduced a factor,

$$\beta = \frac{\frac{1}{u_{as}} + \frac{1}{u_p}}{\frac{1}{c} - \frac{1}{u_p}} \simeq -1 - \frac{u_p}{u_{as}}, \quad (9)$$

which is a merit of figure of frequency-correlated biphotons. The relation $\lim_{L \rightarrow \infty} \sin(xL)/x = \pi\delta(x)$ allows us to reexpress the joint natural spectrum function Φ as

$$\lim_{L \rightarrow \infty} \Phi(\Delta_k L) = \frac{2\pi}{L} \delta(\Delta_k) e^{-i(\Delta_k L/2)}. \quad (10)$$

By substituting Eq. (10) into Eq. (7) and by completing the integrations, this leads to the following two-photon state:

$$\begin{aligned}
 |\Psi\rangle &= A \int d\omega \tilde{E}_p[\omega(1 + \beta)] \chi_{as}^{(3)}(\omega) \hat{a}_s^\dagger(\beta\omega + \varpi_s) \hat{a}_{as}^\dagger \\
 &\quad \times (\omega + \varpi_{as}) |0\rangle.
 \end{aligned} \quad (11)$$

Again, all the slowly varying terms and constants are grouped into A . From Eq. (11), it is obvious that the total spectrum function of the state is a convolution of the probe spectral profile $\tilde{E}_p(\omega)$ and the third-order nonlinear coefficient $\chi_{as}^{(3)}(\omega)$. Moreover, different from the results obtained for the frequency-anticorrelated case [11,19], here, the natural spectrum function cannot be used to further shape the biphoton state. Furthermore, the state (11) is a maximally entangled-photon state and cannot be factorizable.

Before proceeding to Sec. IV, let us add a few discussions about the parameter β . From Eq. (9), we are ready to find that $t_{as} - t_p = \beta(t_s + t_p)$, where t_j is the time for the ω_j field to traverse the atomic ensemble. For simplicity, we look at the case of $\beta = 1$. In such a case, $t_{as} - t_p = t_s + t_p$ implies that, although the Stokes and anti-Stokes photons propagate backward, they are always symmetrically located on each side in reference to the peak of the probe profile (i.e., the regenerated backward-propagating probe pulse) within the atomic gas, as pictorially illustrated in Fig. 2. It is clear that, when $\beta = 1$, it gives the perfect frequency-correlated photons, which are distributed symmetrically around the center of the backward-propagation probe pulse, similar to the case studied in Ref. [7]. In fact, if $\beta \neq 1$, this still gives frequency-correlated biphotons except that the two photons are located unsymmetrically around the center of the regenerated backward-propagating probe profile. For frequency-correlated entangled photons, the condition of $|u_p| > u_{as}$ should be satisfied as indicated from Eq. (9). Here, this implies that $|\Omega_c|$

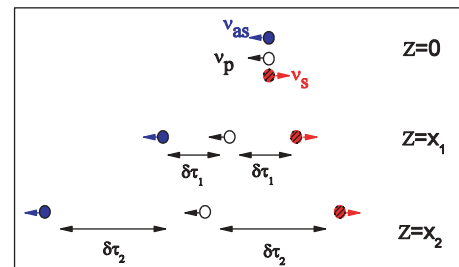


FIG. 2. (Color online) Pictorial illustration of the propagation of frequency-correlated Stokes-anti-Stokes photons relative to the probe photon for $\beta = 1$. Z is the propagation distance inside the atomic gas.

will be less than γ_{41} [i.e., operating in the (ultra-)slow light limit]. The condition $\beta > 0$ greatly loosens the requirement for producing frequency-correlated photons as emphasized in the literature. Here, we note that, for the copropagation case, it is impossible to satisfy the extended-phase-matching condition, since $\beta = (\frac{1}{u_p} - \frac{1}{u_{as}})/(\frac{1}{c} - \frac{1}{u_p}) < 0$, and, hence, no frequency-correlated photons are observable.

IV. COINCIDENCE-COUNTING EXPERIMENT

To study the optical properties of frequency-correlated Stokes and anti-Stokes photons, we examine a simple two-photon temporal correlation experiment as schematically depicted in Fig. 1(b). First, we begin with the single-photon counting measurement, say, detecting anti-Stokes photons. The first-order correlation function is given by

$$G^{(1)} = \langle \Psi | \hat{E}_{as}^{(-)}(\tau_2) \hat{E}_{as}^{(+)}(\tau_2) | \Psi \rangle = \sum_{k'} |\langle 0 | a_{k'} \hat{E}_{as}^{(+)}(\tau_2) | \Psi \rangle|^2, \quad (12)$$

where $\hat{E}_{as}^{(+)}$ refers to the positive-frequency component of the free-space electromagnetic field triggered at detector D_2 . In Eq. (12), $\tau_2 = t_2 - \frac{z_2}{c}$, where z_2 denotes the distance from the output surface of the ensemble to the plane of D_2 and t_2 represents the trigger time. With the use of Eq. (11), one can show that

$$G^{(1)} = B_1 \int d\omega |\chi_{as}^{(3)}(\omega) \tilde{E}_p[\omega(1+\beta)]|^2, \quad (13)$$

where B_1 is a constant. It is clear that the singles counting rate gives a featureless constant, as expected.

Now let us turn to the two-photon coincidence-counting measurement in the low optical-depth regime. For simplicity, we assume that there is no filter placed before detectors D_1 and D_2 . With the help of Eqs. (1) and (11), we are ready to show

$$G^{(2)}(\tau_1, \tau_2) = |\langle 0 | \hat{E}_2^{(+)}(\tau_2) \hat{E}_1^{(+)}(\tau_1) | \Psi \rangle|^2 = B_2 \left| \int d\omega \frac{\tilde{E}_p[\omega(1+\beta)] e^{-i\omega(\beta\tau_1 + \tau_2)}}{(\omega + \Omega_e + i\gamma_e)(\omega - \Omega_e + i\gamma_e)} \right|^2. \quad (14)$$

Here, B_2 is a grouped constant, and $\tau_1 = t_1 - \frac{z_1}{c}$, where z_1 is the distance from the output surface of the gas to D_1 and t_1 is its trigger time. In Eq. (14), we rewrite $\chi_{as}^{(3)}(\omega)$ around its two resonances as done in Ref. [11]. Ω_e is the effective Rabi frequency, and γ_e is the effective dephasing rate. Equation (14) is another important result obtained in this paper. Mathematically, it is a Fourier transform. If the spectrum function of the probe field is given, one can immediately obtain the knowledge of the two-photon temporal correlation. For example, if the input probe field takes a Gaussian profile with bandwidth σ , $\tilde{E}_p(\nu_p) = e^{-\nu_p^2/\sigma^2}$, after some algebra, Eq. (14) becomes

$$G^{(2)}(\tau_1, \tau_2) = B_2 e^{-2\gamma_e(\beta\tau_1 + \tau_2)} \{1 - \cos[2\Omega_e(\beta\tau_1 + \tau_2) - \alpha]\}, \quad (15)$$

with a constant phase $\alpha = 4\Omega_e\gamma_e(1+\beta)^2/\sigma^2$. Again, all the slowly varying terms and constants are absorbed into B_2 .

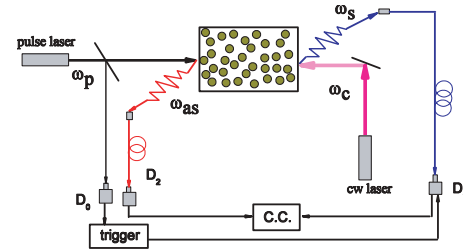


FIG. 3. (Color online) Two-photon coincidence measurement conditioned on the trigger of the input probe pulse.

By changing the Rabi frequency of the control field and the bandwidth of the probe pulse, the range of α is not limited in $(0, 2\pi]$ and can be even greater than 2π . Equation (15) shows that $G^{(2)}$ exhibits damped Rabi oscillations with the period π/Ω_e and the damping rate $2\gamma_e$ due to the two-photon interference between two FWM processes, as reported in Refs. [9,11]. Here, however, the constant phase α distinguishes the current case from previous studies. That is, the two-photon antibunchinglike effect can be switched to the bunchinglike effect by tuning α . Alternatively, the observation of the shifting of the minimum toward $\tau_j > 0$ gives a signature of the detection of frequency-correlated paired photons. Since these narrowband photons have bandwidths typically from megahertz to hundreds of megahertz, the current state-of-the-art single-photon detectors with tens of picosecond timing resolutions are fast enough to resolve each pair directly in the time domain. Therefore, the coincidence-counting rate is simply proportional to $G^{(2)}$. One may notice that two timings appear in Eq. (15). In the experiment, how can one implement the measurement? In fact, one timing can be removed from Eq. (15) by using part of the input probe pulse as a trigger to initiate the coincidence circuit, as shown in Fig. 3. In Fig. 4, we plot two curves of the conditional $G^{(2)}(\tau_2, \tau_1 = 0)$ by setting $(\Omega_e = 1.2\gamma_e, \alpha = \pi/2)$ (dashed line) and $(\Omega_e = 1.2\gamma_e, \alpha = 2\pi)$ (solid line), respectively. For the atomic gas with high optical depth, the situation is closer to the SPDC case [7], which will not be addressed here.

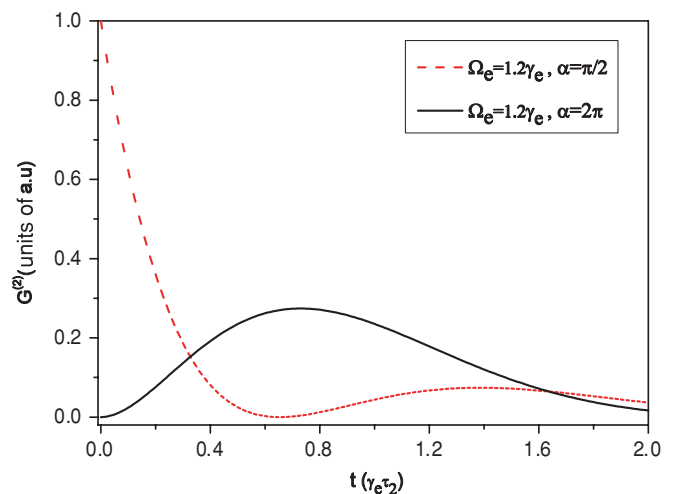


FIG. 4. (Color online) Second-order temporal conditional correlation function $G^{(2)}$ as a function of τ_2 .

V. CONCLUSION

To summarize, we have theoretically studied the generation of frequency-correlated narrowband Stokes-anti-Stokes photons through FWM in a cold atomic system, especially in the low optical-depth region. For simplicity, we take the input probe field as a pulsed laser, while we take the control light as a cw beam. We have extended the condition, which allows us to yield the frequency-correlated paired photons. For the experiment, we proposed performing a two-photon temporal correlation measurement conditioned on the trigger of the probe pulse. Our results show that, by changing the constant phase α , the damped Rabi oscillations can be tuned from the two-photon antibunchinglike effect to the bunchinglike effect. Alternatively, this also provides a signature for the observation of frequency-correlated photons in the experiment. In addition,

our results suggest other evidence for observing backward pulse propagation from the viewpoint of the two-photon correlation measurement. This research could be useful for fields, such as quantum-information science and quantum metrology.

ACKNOWLEDGMENTS

We thank Shengwang Du and Yan-Xiao Gong for useful discussions. J.W. acknowledges the financial support from the 111 Project No. B07026 (China). This work was supported by the National Natural Science Foundations of China under Contracts No. 10904066 and No. 11021403, and the State Key Program for Basic Research of China (Contract No. 2010CB630703). J.W. and M.X. were also partially supported by the National Science Foundation (USA).

-
- [1] Y. H. Shih, *Rep. Prog. Phys.* **66**, 1009 (2003); D. N. Klyshko, *Photons and Nonlinear Optics* (Gordon and Breach, New York, 1988).
 - [2] A. Valencia, A. Ceré, X. Shi, G. Molina-Terriza, and J. P. Torres, *Phys. Rev. Lett.* **99**, 243601 (2007).
 - [3] M. B. Nasr, S. Carrasco, B. E. A. Saleh, A. V. Sergienko, M. C. Teich, J. P. Torres, L. Torner, D. S. Hum, and M. M. Fejer, *Phys. Rev. Lett.* **100**, 183601 (2008).
 - [4] X. Q. Yu, P. Xu, Z. D. Xie, J. F. Wang, H. Y. Leng, J. S. Zhao, S. N. Zhu, and N. B. Ming, *Phys. Rev. Lett.* **101**, 233601 (2008).
 - [5] T. E. Keller and M. H. Rubin, *Phys. Rev. A* **56**, 1534 (1997).
 - [6] O. Kuzucu, M. Fiorentino, M. A. Albota, F. N. C. Wong, and F. X. Kärtner, *Phys. Rev. Lett.* **94**, 083601 (2005).
 - [7] V. Giovannetti, L. Maccone, J. H. Shapiro, and F. N. C. Wong, *Phys. Rev. Lett.* **88**, 183602 (2002); *Phys. Rev. A* **66**, 043813 (2002).
 - [8] V. Giovannetti, S. Lloyd, and L. Maccone, *Phys. Rev. Lett.* **96**, 010401 (2006).
 - [9] V. Balić, D. A. Braje, P. Kolchin, G. Y. Yin, and S. E. Harris, *Phys. Rev. Lett.* **94**, 183601 (2005).
 - [10] S. Du, P. Kolchin, C. Belthangady, G. Y. Yin, and S. E. Harris, *Phys. Rev. Lett.* **100**, 183603 (2008).
 - [11] S. Du, J.-M. Wen, and M. H. Rubin, *J. Opt. Soc. Am. B* **25**, C98 (2008).
 - [12] J.-M. Wen, S. Du, and M. H. Rubin, *Phys. Rev. A* **75**, 033809 (2007); S. Du, J.-M. Wen, M. H. Rubin, and G. Y. Yin, *Phys. Rev. Lett.* **98**, 053601 (2007).
 - [13] J.-M. Wen, S. Du, Y. P. Zhang, M. Xiao, and M. H. Rubin, *Phys. Rev. A* **77**, 033816 (2008).
 - [14] S. Du, J.-M. Wen, and C. Belthangady, *Phys. Rev. A* **79**, 043811 (2009).
 - [15] J. F. Chen, S. Zhang, H. Yan, M. M. T. Loy, G. K. L. Wong, and S. Du, *Phys. Rev. Lett.* **104**, 183604 (2010).
 - [16] J.-M. Wen, Y.-H. Zhai, S. Du, and M. Xiao, *Phys. Rev. A* **82**, 043814 (2010).
 - [17] H. Y. Ling, Y.-Q. Li, and M. Xiao, *Phys. Rev. A* **57**, 1338 (1998).
 - [18] M. Tsang and D. Psaltis, *Phys. Rev. A* **71**, 043806 (2005).
 - [19] J.-M. Wen and M. H. Rubin, *Phys. Rev. A* **74**, 023808 (2006); **74**, 023809 (2006).
 - [20] R. Y. Chiao, *Phys. Rev. A* **48**, R34 (1993).
 - [21] G. M. Gehring, A. Schweinsberg, C. Barsi, N. Kostinski, and R. W. Boyd, *Science* **312**, 895 (2006).
 - [22] S. E. Harris, *Phys. Today* **50**(7), 36 (1997); M. Xiao, Y.-Q. Li, S.-Z. Jin, and J. Gea-Banacloche, *Phys. Rev. Lett.* **74**, 666 (1995).
 - [23] D. A. Steck, [<http://george.ph.utexas.edu/~dsteck/alkalidata/rubidium87numbers.pdf>].
 - [24] M. H. Rubin, D. N. Klyshko, Y. H. Shih, and A. V. Sergienko, *Phys. Rev. A* **50**, 5122 (1994).